A simulation that recapitulates the dynamics of PER-directed colloidal assembly[†]

Cheng-Hung Chou,[‡] Pepijn G. Moerman,[¶] Sikao Guo,[§] Yiben Fu,[§] Margaret E.

Johnson,[§] Yannis Kevrekidis,[‡] and Rebecca Schulman*,[‡]

‡Department of Chemical and Biomolecular Engineering, Johns Hopkins University,
Baltimore, MD 21218, USA

¶Department of Chemical and Chemical Engineering, Eindhoven University of Technology,
Eindhoven, 5612 AE, The Netherlands

§Department of Biophysics, Johns Hopkins University, Baltimore, MD 21218, USA

E-mail: rschulm3@jhu.edu

Abstract

The self-assembly of DNA-coated colloids controlled by enzymatic reactions has the potential to enable the formation of materials with hierarchical organization and switchable configurations. However, the problem of designing such self-assembly is complex, and an effective simulation is necessary to assist in searching for appropriate design protocols. Typical computational methodologies such as molecular dynamics and Brownian dynamics have limited ability to access the long time scales required for these hierarchical self-assembly processes. Here we adopt a particle-based reaction-diffusion algorithm to model the spatial-temporal evolution of hundreds to thousands of micronscale DNA-coated colloid self-assembly process over hours. In order to demonstrate

 $^{^{\}dagger} A$ footnote for the title

the capability of this digital twin, we compared its predicted core-shell assembly process to results from experiments. The model can qualitatively reproduce the core-shell structures observed in experiment by recapitulating the emergence of compositional heterogeneity when delays between distinct assembly times are introduced. These results support the idea that this approach can successfully capture dynamics over long time scales and the appropriate scale of structure formation. We then use the model to explore different protocols for structure evolution, suggesting how this tool can aid in the design of complex self-organization processes.

Introduction

Self-assembly, a fundamental process in nature, plays a crucial role in various fields such as materials science, chemistry, and biology. Understanding the intricate dynamics and pathways of self-assembly systems across a vast parameter space presents a significant challenge. Computational modeling emerges as a powerful tool to tackle this challenge by providing insights into the underlying mechanisms governing self-assembly phenomena. It offers a versatile approach to explore self-assembly processes due to its ability to simulate complex systems and analyze interactions between individual components. Through simulations, we can investigate the aggregation kinetics, thermodynamics, and structural evolution of self-assembling systems with high temporal and spatial resolution ¹

The use of DNA-coated colloids as building blocks holds tremendous promise for designing multi-stage assembly of complex functional material due to their specificity and programma-bility.^{2–7} Encoding responsiveness to assembly protocols into the DNA strands enables the prescription of orthogonal interactions, kinetic pathways, and fine control over structural formation. Additionally, coupling DNA-coated colloidal particles aggregation-disaggregation transitions with enzymatic reactions allows for the creation of far-from-equilibrium dynamic systems across large timescales. The use of external chemical signals and geometric constraints further enables spatial-temporal dynamic control over DNA colloid organization, ^{8,9}

making it possible to tailor specific final aggregate formations by choosing appropriate staged protocols.

One approach for such staged assembly is the autonomous temporal control over DNA-coated colloid arrangements using the Primer Exchange Reaction (PER). ¹⁰ By appending new "sticky" DNA domains onto pre-grafted DNA strands on colloids, the pair interaction between particles can be regulated at different stages. However, designing protocols to achieve a specific assembly outcome using such a protocol presents a challenge. What will be the final structure look like given a set of reactants? Meanwhile, for inverse design, what will be the right types and numbers of particles and assembly protocol given a complex structure formation requirement? To address these questions, computational simulations are necessary to predict the outcome of specific protocols in order to rapidly search for an appropriate protocol.

Simulating kinetic trapping particle assembly over multiple hours is challenging. Typical numerical simulations on DNA-coated colloidal assembly use a potential-based approach, such as Molecular Dynamics (MD) and Brownian Dynamics (BD), which iterate small displacement moves to recapitulate over-damped Langevin equation. The regimes accessible to these methods primarily focus on investigating microscopic morphology in equilibrium and systems of relatively short timescales (less than a minute) as well as small magnitudes (less than a few hundred particles). ^{11–14} However, dynamical non-equilibrium transient self-assembly usually spans hours, which is computationally expensive to model using potential-based approaches. These approaches require tiny iteration steps to integrate particles' motion over a short-ranged pairwise potential landscape. Specifically, the Langevin equation governing the assembly dynamics is stiff because the attraction between particles is short-ranged, requiring a step size much smaller than the timescales of interest. An alternative approach should be applied to help understand the collective emergent behavior on mesoscale across long timescales.

Reaction-Diffusion (RD) approaches are widely used to solve mesoscale problems. De-

terministic continuum Partial Differential Equation (PDE) or stochastic Reaction-Diffusion Master Equation (RDME) approaches, ^{15,16} are suitable for exploring the species concentration field, without considering their geometry of the particle assemblies. However, the macroscopic formation of DNA colloids results from collaborative interactions between individual constituents. Thus, a comprehensive tracking of spatial and structural resolution of each particle is required for assembly modeling. The single-particle Reaction-Diffusion method provides a particle-level resolution depiction for such agent-based modeling, and it has been used to synchronize dynamics in biochemical systems such as protein and cell assembly. ^{17–19}

One approach that successfully describes the reaction dynamic between rigid diffusing particles is the Green's function Reaction Dynamics (GFRD), which is the analytical solution of the Smoluchowski diffusive model with radiation boundaries. For colloidal assembly, Brownian particle coagulation with short-range pairwise interactions can also be represented with the probablitatic Smoluchowski diffusive model. ²⁰ Here, we apply the single-particle Reaction-Diffusion method for studying time-dependent DNA colloid organization with a short-range potential on the mesoscale. In Section 1, we provide a concise overview of the computational methodologies employed in our study. Sections 2.1 and 2.2 delve into the simulations of DNA-coated colloidal aggregation, specifically focusing on the mechanisms driven by primer exchange reactions. Section 2.3 explores the core-shell assembly process, while Section 2.4 investigates various assembly protocols. Our findings demonstrate that the proposed computational approach effectively simulates the macroscopic development of clustering formation over extended iteration steps and long timescales. Additionally, the approach qualitatively captures the dynamic processes involved in the assembly, providing valuable insights into the underlying mechanisms.

Results and discussion

DNA-coated colloidal aggregation driven by Primer Exchange Reactions

The use of PER sequence-editing during a reaction makes it possible to control when particles are able to bind to one another during a reaction by controlling the rate at which a specific sequence domain is appended to strands grafted to particles. ²¹ During a constant-temperature reaction, once enough strands have been converted through this appending (or conversion) process, the particles are able to bind to one another because the melting temperature of the particles exceeds the reaction temperature. ¹⁰ Since the rate of strand conversion is dependent on the concentration of a catalyst hairpin that acts as a template from which the appended sequence is copied, the time at which the particle binding begins can be chosen by choosing the concentration of the hairpin.

We sought to develop a simulation process that could, by recapitulating the results of PER-regulated particle binding processes, make it possible to design processes for assembling particular products in silico. As a first step, we developed a procedure for quantifying the dynamics of PER-regulated particle aggregation so that these dynamics could be compared with those in our simulations.

To measure the rate of example PER-regulated particle binding processes, we prepared mixed suspensions of single-strand DNA-coated polystyrene particles, consisting of one type of precursor particle and one type of co-assembler particle, both with a diameter of $1\mu m$ (sequences are in SI I). ²¹ We dispersed 0.1wt% each of the precursor and co-assembler in a $10mm \cdot 1mm \cdot 100\mu m$ -sized capillary tube along with various concentration of PER templates at $30^{\circ}C$. Precursors present the sequence A; this sequence is converted into sequence AI, using template A'I', so after a sufficient extent of conversion, the precursor particles can bind to the co-assembler particles via the hybridization of the sequence domain I to the complementary domain I' on the co-assembler particles.

We measured the state of particles' aggregation over time using bright-field microscopy with a 60x objective having a 1.42 numerical aperture. The particles sediment in their aqueous solution, so that micrographs of the fluid near the bottom of the glass capillary capture the state of the pseudo-2D aggregation process. We extracted from these images the sizes s(t) (scalars), and the fractal dimension $f_d(t)$ (scalar) of clusters at different reaction times.

To investigate the dynamics of cluster aggregation, it is essential to examine the relationship between the binding rate of particles and the evolution of size s(t), and the fractal dimension $f_d(t)$ of the clusters. The size evolution of particle clusters during coagulation can be effectively described using the Smoluchowski coagulation equation, as shown in Eq. (1).²²

$$\frac{dN_k}{dt} = \frac{1}{2} \sum_{i=1}^{k-1} K_{i,k-1} N_i N_{k-i} - N_k \sum_{i=1}^{\infty} K_{ik} N_i$$
 (1)

In this context, the coagulation kernel K is a function of binding rate, which directly influences the rate at which particles coalesce. Moreover, the fractal dimension f_d a measure of the complexity and branching of random aggregates, is also dependent on the binding rate. This relationship highlights that both the size and fractal properties of 3D aggregates can be modulated by adjusting k, with the fractal characteristics of these aggregates showing a correlation with their 2D projection images.²³

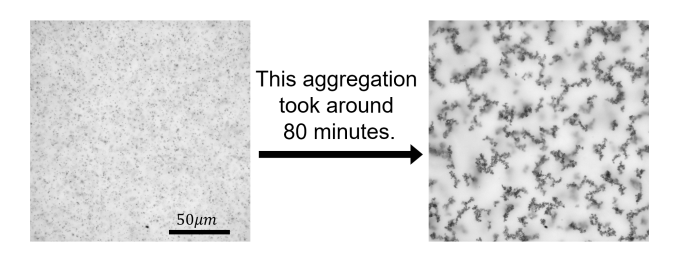


Figure 1: Micrographs of experiments characterizing DNA-coated colloidal aggregation driven by PER. Left: micrograph of particles just after their addition to a slide. Right: micrograph captured 80 minutes after the start of aggregation. Details of experimental protocol and movies are in SI II

To extract cluster size and fraction dimension from micrographs, the images were first binarized using Otsu thresholding²⁴ to identify each cluster's location, followed by image segmentation to refine the property (size s(t), and fractal dimension $D_f(t)$) of the individual cluster. Specifically, by converting the image into a binary format, where each pixel is either black or white with thresholding, image segmentation techniques can then be applied to separate different regions or clusters within the image. The total sizes of clusters s(t) was determined by taking the weighted arithmetic mean of size of clusters. The fractal dimensions $f_d(t)$ were estimated using box-counting method. ²⁵

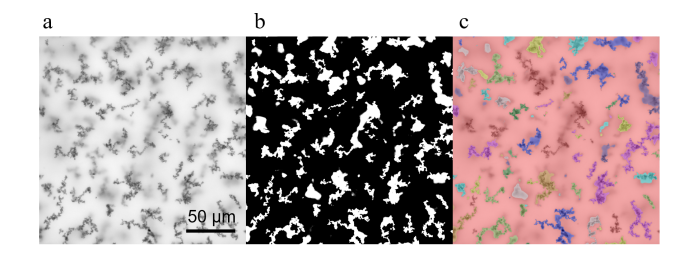


Figure 2: Processing microscope images to extract aggregation state. (a) a sample microscope image of PER controlled assembly (b) a binarized image produced using Otsu thresholding (c) individual cluster refined using image segmentation. Each cluster is shown in a different color to indicate cluster identity.

Colloidal aggregation modeling using stochastic Single-particle Reaction-Diffusion algorithm

To recapitulate the aggregation dynamic of DNA-coated colloid, we utilized the Non-equilibrium Reaction-Diffusion Self-assembly simulator (NERDSS) to simulate the aggregation. ^{17–19} This simulator employs the Free-propagator reweighting (FPR) algorithm, derived from Green's function Reaction-Diffusion, which accurately captures the reacting dynamics between colliding particles. ^{19,26} It iterates stochastic, structure-resolved Smoluchowski Reaction-Diffusion at a single-particle level, which is customizable with user-defined particles, reactions, and systems.

This approach allows for large time-steps and precise dynamics by breaking down the

many-body system into a series of two-body problems and computing the binding probability using the probabilistic Smoluchowski diffusive model.

A physical description was established to model the aggregation of DNA-coated colloidal particles. We design $1\mu m$ sized particles with 12 non-specific binding patches (a particle can bind up to 12 particles geographically) without a fixed binding orientation. To account for the excluded volume effect, the patches were consolidated to the particle center and have a certain binding distance between them (d=2r). For particles' diffusion. translational and rotational diffusion constants are estimated with Stokes-Einstein equation at $30^{\circ}C$: $D_T = 0.55 \mu m^2 s^{-1}, D_r = 1.66 \cdot 10^{-6} radians^2 \mu m^{-1}$ (see (see SI.I).²⁷ Each particles diffused as a rigid body and its displacement was updated using translational Brownian motion, i.e. $x(t+t) = x(t) + \sqrt{2D_T \cdot \Delta t} \cdot R$, along 3 axes, where R is a random variable drawn from the standard normal distribution. Since the particles settle due to gravitational force, we iterate the displacement with additional settling displacement term $-37.4ms^{-1} \cdot \Delta t$ in z direction (see SI.II). We also assumed that the settling velocity is the same for all clusters and particles, despite the smaller hydrodynamic drag force per particle experienced by clusters. We assumed that this deviation would be insignificant, since the error in settling time is negligible compared to the timescale of our interest. For rotational diffusion, a cluster rotates along the 3 axes with an angle $\theta_t = \sqrt{2D_T \cdot \Delta t} \cdot R^{17}$

Regarding the transport properties of complexes, the diffusions were inhibited with increasing size, reflecting the assumption that the hydrodynamic radius of the cluster is the sum of its components. The diffusion constants of complexes are thus determined with $D_T = \left[\sum_{i=1}^N D_{Ti}^{-1}\right]^{-1}$, $D_R = \left[\sum_{i=1}^N D_{Ri}^{-1/3}\right]^{-3}$, where D_{Ti} , D_{Ri} are the translational and rotational diffusion constant for each constituent of the complexes. New trajectory positions are refused and reiterated if violating excluded volume. ¹⁷

One major hypothesis we have regarding the aggregation dynamics is that there is a fixed binding rate and binding constant, denoted as k_b that govern the overall aggregation process. For aggregation description, the binding reactions were enumerated for every pair of

patches using rule-based modeling. ²⁸ Since the aggregation-disaggregation transition is sharp with increasing DNA coverage conversion by PER, ¹⁰ the binding affinity regulation can be generalized as a step function. ²⁹ To model irreversible assembly, we sampled aggregation with a fixed microscopic binding constant k_b ranging from 1 to $10^6 nm^2 \cdot \mu s^{-1}$ as well as unbinding constant $k_d = 0s^{-1}$ (see SI.III). For numerical step selection, we chose the step size $\Delta t = 20ms$ for all simulation (see SI.IV). To reproduce the experimental pseudo-2D aggregation, we randomly assigned 2000 precursor and 2000 co-assemble particles in a simulated box boundary of size $100 \times 100 \times 100 \mu m$ (see SI.V). We set each particle concentration to 0.1wt% in line with the experimental setup. After allowing the particles to reach sedimentation equilibrium for 60 minutes, we initiated the binding affinity between them and allows for the random aggregation, as Fig. ?? shows. The trajectory of each particle was monitored at 1-minute intervals.

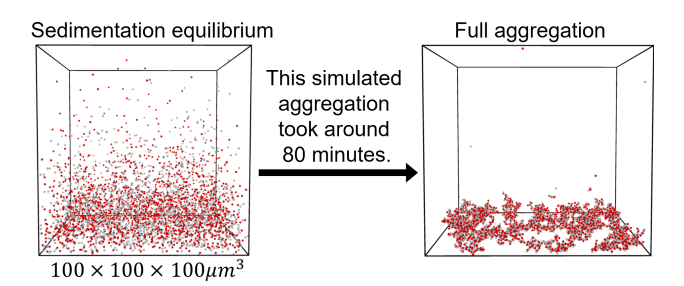


Figure 3: Simulated colloidal aggregation: particles start to form pseudo-2D random aggregate after reaching sedimentation equilibrium.

To compare our simulations with the experimental results, we created simulated bright-field microscope images and extracted the parameters, including size, fractal dimension and ratio of area. We took the bottom spacing of $10\mu m$ of the particle trajectory and created 2D projection images of pseudo-2D random aggregates, as Fig. 4 shows. The images were convoluted with Gaussian blur approximation with $\sigma = 0.62$. We then merged images from four random runs with random rotations of 0° , 90° , 180° , and 270° to create simulated microscope images of 100 runs with the same scale as the experimental ones. We conducted a similar analysis to collect the median of critical parameters from the simulated images.

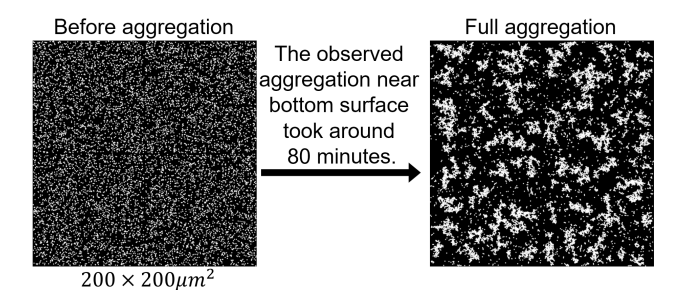


Figure 4: 2D projection image of simulated colloidal aggregation

One primary question rise: within which range of binding constants should we make our selection? First, we investigate the pseudo-2D cluster's height across a range of binding constants k_b . From Fig. ??, our findings indicate that when k_b is equal to or greater than 500, the clusters' height remains approximately unchanged. The phenomena happens because we have limited amount of particles. Thus, we constraint k_b from 1 to $500nm^2 \cdot \mu s^{-1}$.

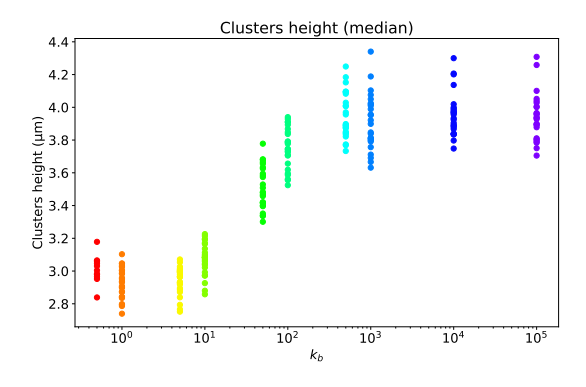


Figure 5: c luster height distribution with various effective binding constant k_b

Next, we examine how the value of k_b influences critical parameters such as size evolution and fractal dimension. Fig. 6 shows the size evolution profile s(t) as a function of various effective binding constant k_b . The simulations have the similar trending with the experimental aggregation. Fig. 7 shows the fractal dimension profile $f_d(t)$. Simulations with display fractal properties are similar to the experimental results. However, it is worth noting that both simulations and experiments exhibit significant variance among sample runs. Therefore, further investigation is necessary to thoroughly examine the aggregation dynamics.

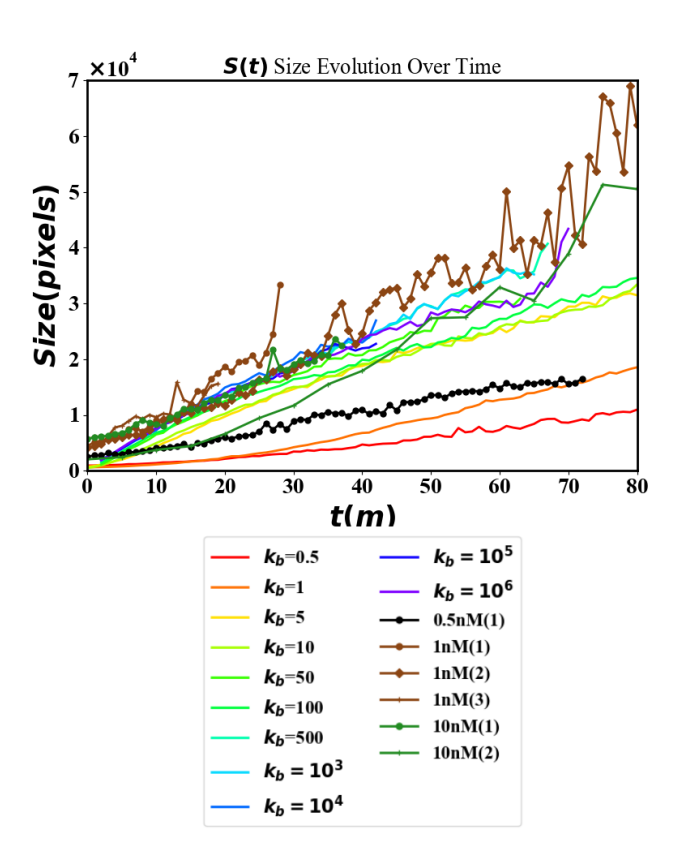


Figure 6: Size evolution S(t) as a function of various k_b in simulation and various concentration of catalytic template in experiments. Results shows that the trend from both experiment, and modeling are similar.

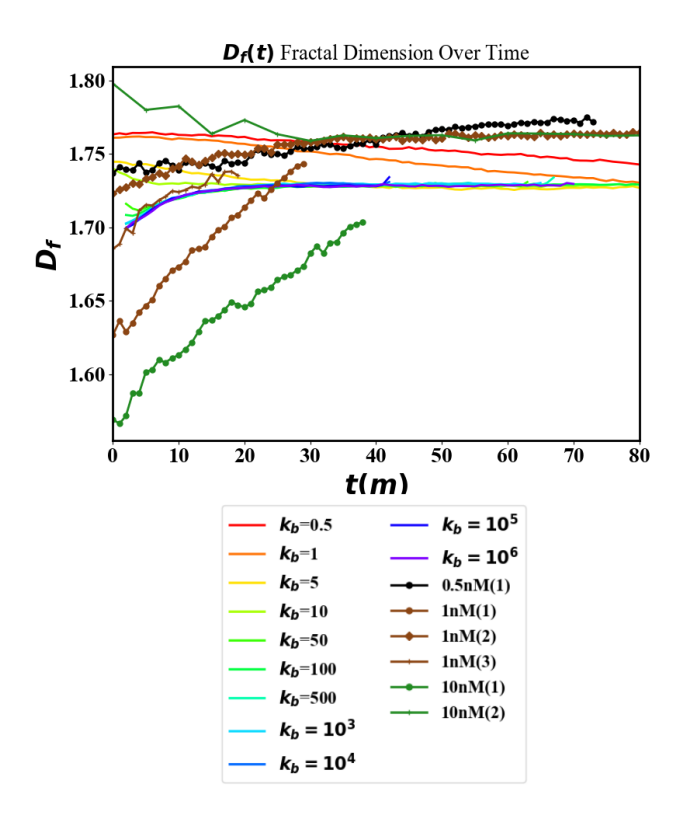


Figure 7: Fractal dimension over time as a function of various k_b in simulation and various concentration of catalytic template in experiments. Results show that the trend from both experiment, and modeling are similar.

Multi-component autonomous aggregation with pre-defined rules

To showcase the versatility of our PER self-assembly framework, we have demonstrated a sequential assembly scenario: a core-shell formation. We prepared a single feedstock of DNA colloids: a mixed suspension of two types of precursors (labeled with fluorescent magenta and green dyes) and one type of co-assembler particles, all of which are $1\mu m$ diameter polystyrene particles with single-strand DNA pre-coated on their surface. We dispersed 0.1wt% of each component in $100\mu m$ -sized spherical water droplets along with various PER templates at 30°C. Precursors magenta were converted into AI using template A'I', and precursors green were converted into BI using template B'I'. The precursors bind to the co-assembler particles via complementary strand I' on the co-assembler, resulting in the formation of core-shell structures. The conversion rate is a function of reaction time and catalytic template concentration, allowing us to engineer the interval between the two stages of assembly. Each activation occurs in tandem, but the binding affinity of magenta particles is faster than that of green particles. As a result, we observe precursor magenta and co-assembler forming the core structure at the first stage with a 1nm template A'I', followed by shell formation resulting from the aggregation between precursor green and co-assembler with a 0.05nm template B'I'. The predefined rules can thus be tailored by prescribing various amount and type of catalytic template. To demonstrate the wide-ranging capabilities of our design, we have examined kinetic arrest structures using different timestaged protocols. Specifically, we design core-shell structures with various compositional heterogeneity by changing the time delay between two stages. Fig. ?? displays the sketch and experimental and preliminary results of the core-shell gelation experiment.

Our aim is to create a predictive modeling for DNA colloid sequential assembly. Initially, we randomly place 1,000 of each precursor and co-assembler particle (equivalent to 0.1wt%) within a $100\mu m$ -diameter spherical boundary. At t=100 minutes, we initiate the binding affinity between precursor magenta and co-assembler to simulate the first stage of core formation. We then activate the binding affinity between green particles and co-assembler at

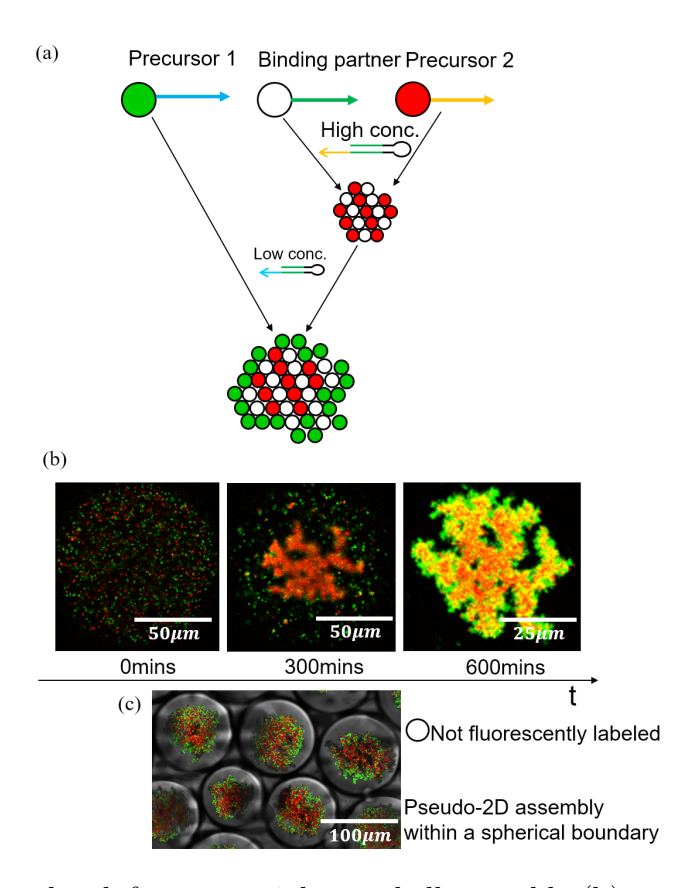


Figure 8: (a) Diagram sketch for sequential core-shell assembly (b) snapshots from sequential assembly experiment over time (c) The assembly happened within spherical water droplet microchambers.

t = 300 minutes to simulate shell formation. Fig. ?? displays snapshots of the modeling process at different stages.

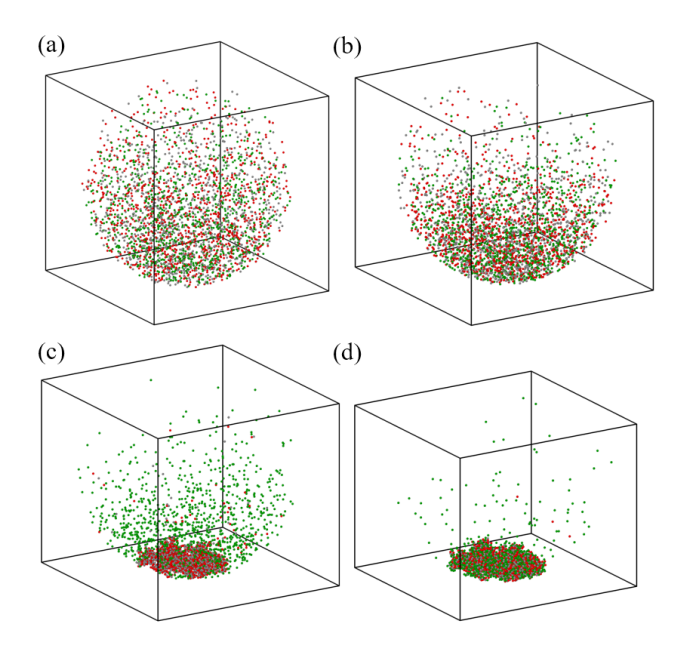


Figure 9: Snapshots from sequential assembly simulation (a) at t=0 min (b) at 100 minutes reaching sedimentation equilibrium (c) at t=300 minutes, particles fall to the bottom and form core structure while the monomer green are still dispersed in the system (d) at t=600 minutes, shell formation happens from the outside of the complex.

Our objective is to replicate the macroscopic organization achieved in multi-component sequential assembly. We choose $k_b = 1nm^2 \cdot \mu s^{-1}$ as the effective binding constant. To validate whether our modeling framework can recapitulate the dynamic behavior of sequential assembly, we have investigated the effect of time delay between assembly stages on compositional heterogeneity. By varying the time delay between the first two stages of assembly, we create structures with different degrees of compositional heterogeneity. For example, a well-mixed structure forms with no time delay between stages, while a 200-minute time delay results in a two-layered core-shell gelation in both the experiment and modeling.

To facilitate the comparison between our computational model and the sequential assembly experiment, we have devised a mathematical protocol aimed at transforming the high-dimensional structure into lower-dimensional images. Specifically, we employ confocal imaging techniques to segment the positional profiles of simulated particles horizontally

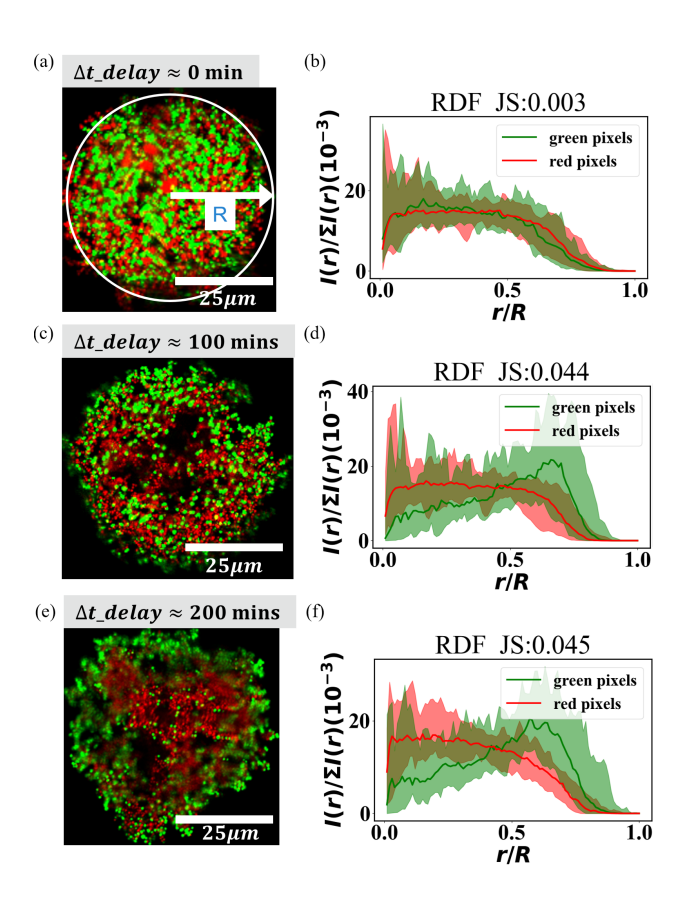


Figure 10: Compositional heterogeneity of sequential assembly with various time delay for experiments. Figures are non-linearly enhanced by ImageJ for visualization.

across subframes ranging from $4\mu m$ to $7\mu m$ subframes with intervals of $1\mu m$. These segmented profiles are then projected onto a single image comprising $100 \cdot 100$ pixels, with intensity values linearly stretched.

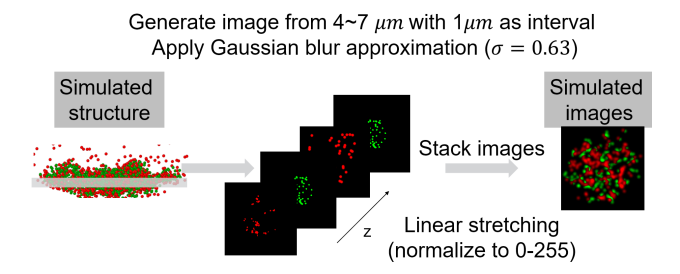


Figure 11: To create simulated confocal images, we compress images taken at various z from $4\mu m$ to $7\mu m$ and compress then into a single image with linear stretching on intensities.

We then compare these images with the confocal images obtained from the sequential assembly experiments, and measure the compositional heterogeneity. We determine radial distribution function (RBF) of red and green pixels. The heterogeneity is then quantified by measuring the Jensen-Shannon divergence (JSD) between two median distribution of RDF of approximate 25 samples. Fig. 10 and Fig. 12 displays structures with different compositional heterogeneity, resulting from varying the time delay between stages in both the modeling and experiments.

In order to demonstrate the statistically significant difference between experiments and simulations, we employ bootstrapping to establish 95% confidence intervals and assess the variability in our findings. As Fig. 13 shows, results show that in both simulations and experiments, for those dataset with time delay t=0m has statistically significant difference between t=100m and t=200m.

Assembly design protocol exploration

Our particle assembly simulator offers a versatile platform for exploring a range of design protocols. One compelling scenario is that we demonstrate a ring formation. Initially, we prepare 3000 particles with a composition of W:R:B = 3:1:3, where the core accounts for

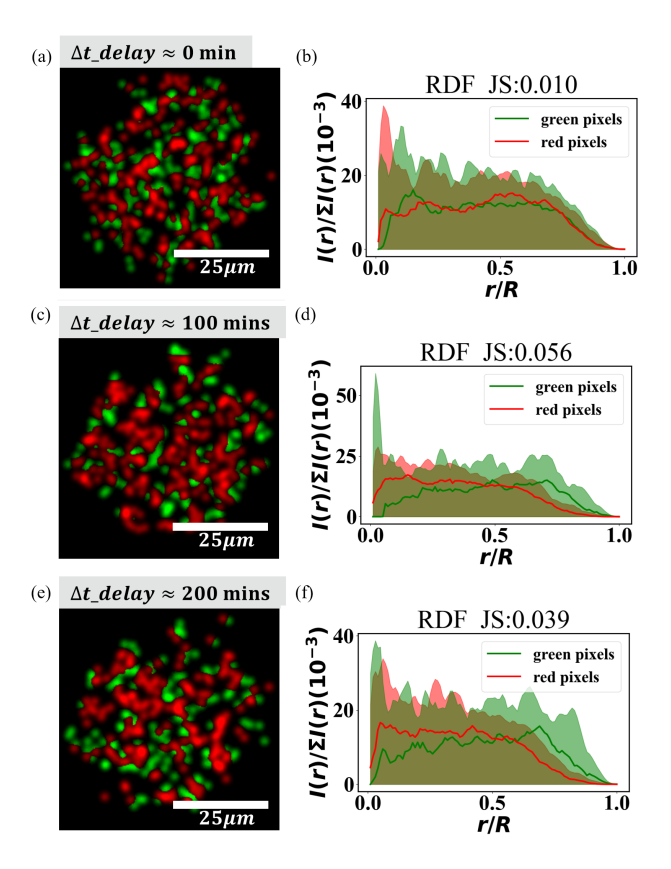


Figure 12: Compositional heterogeneity of sequential assembly with various time delay for simulations. Figures are non-linearly enhanced by ImageJ for visualization.

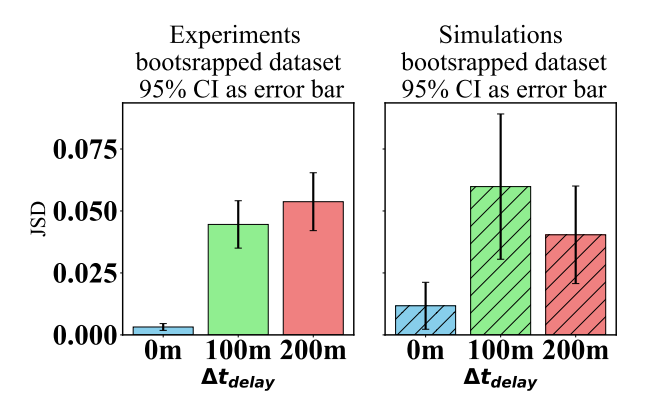


Figure 13: Compositional heterogeneity of sequential assembly with various time delay for experiments. The bar plot with 95% confidence interval as error bar shows the quantitative disparity between time delay t = 0m and t = 100m/t = 200m with statistical significance.

40% red and 60% white, while the shell consists of 60% green and 40% white. The core and shell have radii of 3 and 7, respectively. As Fig. 14 shows, initially bound together, the particles have their core subsequently removed, leaving behind the ring structure. This process allows users to investigate intricate design principles inherent in particle assembly, enabling a deeper understanding of assembly dynamics and structural formation.

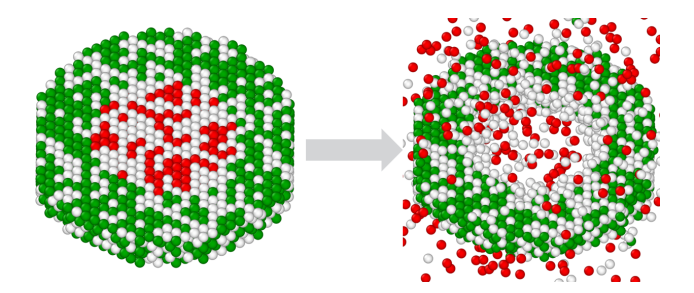


Figure 14: Ring formation before and after: initially, the core-shell structure was bound together, and subsequently, the core was removed, leaving the ring behind.

Conclusion

In conclusion, computational modeling plays a pivotal role in advancing our understanding of self-assembly phenomena by providing mechanistic insights into dynamic behaviors, aggregation dynamics, and pathway exploration across diverse parameter spaces. We have developed a computational model of DNA-coated colloid kinetical trapping formation using structured resolved Single-particle Reaction-Diffusion algorithm. This approach is capable of numerically simulating self-assembly over large length and time scales. We have demonstrated our modeling could recapitulate the colloidal clustering that has a similar size evolution profile s(t), and fractal dimensions f_d . We have also demonstrated the qualitative trend agreement in terms of increasing heterogeneity and delay time. This enables us to unravel the complexities of self-assembly processes, guiding the design of functional colloid with tailored properties and applications.

Regarding the physical rules in the binding probability estimation, the primary question is that if the Smoluchowski diffusive model is still exact and accurate enough for our pseudo2D assembly simulation. That is, the binding probabilities assume only pure Smoluchowski diffusive dynamics between a pair of particles, so that assumption is violated when there is a settling term in particles' motion. However, since we assume all particles and clusters have the same settling velocity, we can consider them in a moving coordinate system and derive its binding probability with Smoluchowski model. Apart from this, it's beyond our capability to measure the exact binding constant from experiment. Instead, we approximate the binding kinetics with a fixed binding constant, and we still can reproduce the macroscopic organization. Hence, the assumption has trivial effect on the assembly pathway in the simulation.

One challenging part in simulation is the estimation of the transport properties of complex clusters. That is, the rotational diffusion constant is hard to estimate for a pseudo-2D cluster formation with sedimentation. For the sake of simplicity, we assume that clusters have the same properties as a 3D spherical object. However, it remains a question how rotational deviation might affect the assembly pathway and whether it should be taken into consideration for a more accurate understanding of the process.

The effect of hydrodynamics is not considered in the modeling, in which particles motion have propagation effect on one another and might affect the overall assembly pathway. It is beyond our capability to estimate the exact hydrodynamics for every constituent over time, considering that each monomer or complex have their distinct geometry and diffusivity. Meanwhile, it would also be computationally costly to compute the many-body hydrodynamics in a large-scale regime. Although the hydrodynamics is not covered in the modeling, the results still show that our simulator is still capable of generalizing the assembly dynamics.

Acknowledgement

We thank Yiben Fu, Sikao Guo, and Prof. Margaret Johnson for discussion and technical support on NERDSS simulator. We acknowledged funding from the Hopkins Extreme Materials Institute (HEMI). This work was carried out at the Advanced Research Computing at Hopkins (ARCH) core facility (rockfish.jhu.edu), which is supported by the National Science Foundation (NSF) grant number OAC1920103.

Supporting Information Available

A listing of the contents of each file supplied as Supporting Information should be included. For instructions on what should be included in the Supporting Information as well as how to prepare this material for publications, refer to the journal's Instructions for Authors.

The following files are available free of charge.

• Filename: brief description

• Filename: brief description

References

- (1) Orsi, M. Self-assembling Biomaterials; Elsevier, 2018; pp 305–318.
- (2) Wang, Y.; Wang, Y.; Zheng, X.; Ducrot, É.; Yodh, J. S.; Weck, M.; Pine, D. J. Crystallization of DNA-coated colloids. *Nature communications* **2015**, *6*, 7253.
- (3) Casey, M. T.; Scarlett, R. T.; Benjamin Rogers, W.; Jenkins, I.; Sinno, T.; Crocker, J. C. Driving diffusionless transformations in colloidal crystals using DNA handshaking. *Nature communications* **2012**, *3*, 1209.
- (4) He, M.; Gales, J. P.; Ducrot, É.; Gong, Z.; Yi, G.-R.; Sacanna, S.; Pine, D. J. Colloidal diamond. *Nature* **2020**, *585*, 524–529.
- (5) Ducrot, É.; He, M.; Yi, G.-R.; Pine, D. J. Colloidal alloys with preassembled clusters and spheres. *Nature materials* **2017**, *16*, 652–657.

- (6) Todhunter, M. E.; Jee, N. Y.; Hughes, A. J.; Coyle, M. C.; Cerchiari, A.; Farlow, J.; Garbe, J. C.; LaBarge, M. A.; Desai, T. A.; Gartner, Z. J. Programmed synthesis of three-dimensional tissues. *Nature methods* 2015, 12, 975–981.
- (7) Hecht, F. M.; Bausch, A. R. Kinetically guided colloidal structure formation. *Proceedings of the National Academy of Sciences* **2016**, *113*, 8577–8582.
- (8) Dehne, H.; Reitenbach, A.; Bausch, A. Transient self-organisation of DNA coated colloids directed by enzymatic reactions. *Scientific Reports* **2019**, *9*, 1–9.
- (9) Dehne, H.; Reitenbach, A.; Bausch, A. Reversible and spatiotemporal control of colloidal structure formation. *Nature Communications* **2021**, *12*, 6811.
- (10) Moerman, P. G.; Fang, H.; Videbæk, T. E.; Rogers, W. B.; Schulman, R. A simple method to reprogram the binding specificity of DNA-coated colloids that crystallize. arXiv preprint arXiv:2206.00952 2022,
- (11) Lee, Y. K.; Li, X.; Perdikaris, P.; Crocker, J. C.; Reina, C.; Sinno, T. Hydrodynamic and frictional modulation of deformations in switchable colloidal crystallites. *Proceedings of* the National Academy of Sciences 2020, 117, 12700–12706.
- (12) Jenkins, I. C.; Crocker, J. C.; Sinno, T. Interaction heterogeneity can favorably impact colloidal crystal nucleation. *Physical Review Letters* **2017**, *119*, 178002.
- (13) Scarlett, R. T.; Crocker, J. C.; Sinno, T. Computational analysis of binary segregation during colloidal crystallization with DNA-mediated interactions. The Journal of chemical physics 2010, 132, 234705.
- (14) Di Michele, L.; Varrato, F.; Kotar, J.; Nathan, S. H.; Foffi, G.; Eiser, E. Multistep kinetic self-assembly of DNA-coated colloids. *Nature communications* **2013**, *4*, 2007.
- (15) Malek-Mansour, M.; Houard, J. A new approximation scheme for the study of fluctuations in nonuniform nonequilibrium systems. *Physics Letters A* **1979**, *70*, 366–368.

- (16) Stundzia, A. B.; Lumsden, C. J. Stochastic simulation of coupled reaction-diffusion processes. *Journal of computational physics* **1996**, *127*, 196–207.
- (17) Guo, S.; Sodt, A. J.; Johnson, M. E. Large self-assembled clathrin lattices spontaneously disassemble without sufficient adaptor proteins. *Biophysical Journal* **2022**, *121*, 331a.
- (18) Varga, M. J.; Fu, Y.; Loggia, S.; Yogurtcu, O. N.; Johnson, M. E. NERDSS: a nonequilibrium simulator for multibody self-assembly at the cellular scale. *Biophysical Journal* **2020**, *118*, 3026–3040.
- (19) Johnson, M. E. Modeling the Self-Assembly of Protein Complexes through a Rigid-Body Rotational Reaction–Diffusion Algorithm. *The Journal of Physical Chemistry B* **2018**, *122*, 11771–11783.
- (20) Hammond, A. Coagulation and diffusion: A probabilistic perspective on the Smoluchowski PDE. **2017**,
- (21) Moerman, P. G.; Chou, C.-H.; Videbæk, T. E.; Rogers, W. B.; Schulman, R. A DNA-encoded recipe to direct multi-stage colloidal assembly. *Manuscript in preparation* **2024**,
- (22) Smoluchowski, M. Mathematical theory of the kinetics of the coagulation of colloidal solutions. Z. Phys. Chem. 1917, 92, 129–168.
- (23) Wang, R.; Singh, A. K.; Kolan, S. R.; Tsotsas, E. Fractal analysis of aggregates: Correlation between the 2D and 3D box-counting fractal dimension and power law fractal dimension. *Chaos, Solitons & Fractals* **2022**, *160*, 112246.
- (24) Liu, D.; Yu, J. Otsu method and K-means. 2009 Ninth International conference on hybrid intelligent systems. 2009; pp 344–349.
- (25) Wang, R.; Singh, A. K.; Kolan, S. R.; Tsotsas, E. Investigation of the Relationship

- between the 2D and 3D Box-Counting Fractal Properties and Power Law Fractal Properties of Aggregates. Fractal and Fractional 2022, 6, 728.
- (26) Johnson, M. E.; Hummer, G. Free-propagator reweighting integrator for single-particle dynamics in reaction-diffusion models of heterogeneous protein-protein interaction systems. *Physical Review X* **2014**, *4*, 031037.
- (27) Hunter, R. J. Foundations of colloid science; Oxford university press, 2001.
- (28) Faeder, J. R.; Blinov, M. L.; Goldstein, B.; Hlavacek, W. S. Rule-based modeling of biochemical networks. *Complexity* **2005**, *10*, 22–41.
- (29) Dreyfus, R.; Leunissen, M. E.; Sha, R.; Tkachenko, A.; Seeman, N. C.; Pine, D. J.; Chaikin, P. M. Aggregation-disaggregation transition of DNA-coated colloids: Experiments and theory. *Physical Review E* 2010, 81, 041404.

TOC Graphic

Some journals require a graphical entry for the Table of Contents. This should be laid out "print ready" so that the sizing of the text is correct. Inside the tocentry environment, the font used is Helvetica 8 pt, as required by *Journal of the American Chemical Society*.

The surrounding frame is 9 cm by 3.5 cm, which is the maximum permitted for *Journal of the American Chemical Society* graphical table of content entries. The box will not resize if the content is too big: instead it will overflow the edge of the box.

This box and the associated title will always be printed on a separate page at the end of the document.